Available online at www.sciencedirect.com

SCIENCE DIRECT®

EPSL

Earth and Planetary Science Letters 220 (2004) 157–174

www.elsevier.com/locate/epsl

Sand petrology and focused erosion in collision orogens: the Brahmaputra case

Eduardo Garzanti[a,*], Giovanni Vezzoli[a], Sergio Andò[a], Christian France-Lanord[b], Sunil K. Singh[c], Gavin Foster[d]

[a] *Dipartimento di Scienze Geologiche, Università di Milano-Bicocca, 20126 Milano, Italy*
[b] *CRPG-CNRS, 15, Rue Notre Dame Pauvres, 54501 Vandoeuvre-les-Nancy, France*
[c] *Physical Research Laboratory, Navrangpura, Ahmedabad 380 009, India*
[d] *University of Bristol, Department of Earth Sciences, Queens Road, Bristol BS8 1RJ, UK*

Received 16 June 2003; received in revised form 11 December 2003; accepted 5 January 2004

Abstract

The high-relief and tectonically active Himalayan range, characterized by markedly varying climate but relatively homogeneous geology along strike, is a unique natural laboratory in which to investigate several of the factors controlling the composition of orogenic sediments. Coupling of surface and tectonic processes is most evident in the eastern Namche Barwa syntaxis, where the Tsangpo–Siang–Brahmaputra River, draining a large elevated area in south Tibet, plunges down the deepest gorge on Earth. Here composition of river sands changes drastically from lithic to quartzofeldspathic. After confluence with the Lohit River, draining the Transhimalayan-equivalent Mishmi arc batholiths, sediment composition remains remarkably constant across Assam, indicating subordinate contributions from Himalayan tributaries. Independent calculations based on petrographical, mineralogical, and geochemical data indicate that the syntaxis, representing only $\sim$4% of total basin area, contributes 35 ± 6% to the total Brahmaputra sediment flux, and $\sim$20% of total detritus reaching the Bay of Bengal. Such huge anomalies in erosion patterns have major effects on composition of orogenic sediments, which are recorded as far as the Bengal Fan. In the Brahmaputra basin, in spite of very fast erosion and detrital evacuation, chemical weathering is not negligible. Sand-sized carbonate grains are dissolved partially in mountain reaches and completely in monsoon-drenched Assam plains, where clinopyroxenes are selectively altered. Plagioclase, instead, is preferentially weathered only in detritus from the Shillong Plateau, which is markedly enriched in microcline. Most difficult to assess is the effect of hydraulic sorting in Bangladesh, where quartz, garnet and epidote tend to be sequestered in the bedload and trapped on the coastal plain, whereas cleavable feldspars and amphiboles are concentrated in the suspended load and eventually deposited in the deep sea. High-resolution petrographic and dense-mineral studies of fluvial sands provide a basis for calculating sediment budgets, for tracing patterns of erosion in mountain belts, and for better understanding the complex dynamic feedback between surface processes and crustal-scale tectonics.

* Corresponding author. Tel.: +39-2-64484338; Fax: +39-2-64484273.
E-mail addresses: eduardo.garzanti@unimib.it (E. Garzanti), cfl@crpg.cnrs-nancy.fr (C. France-Lanord), sunil@prl.ernet.in (S.K. Singh), g.l.foster@bristol.ac.uk (G. Foster).

0012-821X/04/$ – see front matter © 2004 Elsevier B.V. All rights reserved.
doi:10.1016/S0012-821X(04)00035-4

Keywords: Himalaya; Namche Barwa syntaxis; climate; relief; modern sands; bulk petrography; dense minerals; sediment budgets

1. Introduction

The Himalayan belt, characterized by extreme elevation and relief, is subject to severe erosion and represents the most important single source of terrigenous sediments on Earth [1]. The immense mass of detritus produced exceeds by far the storage capacity of the associated foreland basin, and after long-distance fluvial to turbiditic transport accumulates in huge submarine fans on Indian Ocean crust [2,3].

The Himalaya represents a unique natural laboratory in which to investigate how sediment composition reflects the interaction between surface and lithospheric processes [4,5]. Rainfall, which directly controls erosion potential and sediment flux [6], varies considerably across the belt, both from north (as low as 0.1 m/yr in arid Tibet) to south (several m/yr in north Indian rain forests [7]), and from west (basin-wide average 0.4 m/yr for the Indus) to east (basin-wide average 1.75 m/yr for the Brahmaputra). As a consequence, average annual sediment yields increase sharply eastward, from <500 tons/km^2 for the Indus to $\sim$1800 tons/km^2 for the Brahmaputra, which is the big-river basin with the highest denudation rates on Earth (0.69 mm/yr [8]). In spite of a much smaller catchment area than the Indus and the Ganga, the Brahmaputra has a significantly larger sediment discharge (suspended load 540–1157 million tons/yr), surpassed only by the Huanghe and the Amazon [9,10].

Notwithstanding the huge detrital volumes involved [11], the composition of sediments carried by the Brahmaputra and its tributaries is unknown, except for sparse petrographic and mineralogical information on the Ganga and Brahmaputra rivers in Bangladesh [12,13]. Only Bengal Fan turbidites have been accurately studied both petrographically [14] and mineralogically [15–17].

The erosion distribution in the Brahmaputra basin has been recently investigated by using bulk-sediment chemistry and Sr and Nd isotopic tracers [18]. In the present work we carry out, with similar and complementary aims, petrographic and mineralogical analyses on the same sample set. Our principal goals are:

- To document composition of sand-sized detritus carried by the Tsangpo–Siang–Brahmaputra River and its tributaries, thus providing new constraints on collision orogen provenance [19].
- To investigate how relief, erosion patterns, chemical weathering, and hydraulic sorting influence petrography and mineralogy of orogenic detritus.
- To show that high-resolution petrographic and dense-mineral studies represent an effective independent way to calculate sediment budgets. These estimates can be integrated with those obtained with geochemical methods [18,20], in order to assess erosion distribution and sediment fluxes from the Himalayan belt.

2. Materials and methods

2.1. Sampling and analytical procedures

Bedload sands (more suitable than finer-grained suspended load for petrographic investigation) were sampled on active bars of the Brahmaputra and its tributaries from 1999 to 2002, both during and after the monsoon season. Duplicate samples of several major-river sediments (unfortunately not including the Siang) helped us to minimize variations related to seasonal transport modes. Samples are very fine- to medium-grained sands; only Shillong tributaries carry coarse-grained sands. In order to identify the signatures of each major structural domain (e.g., Greater Himalaya, Lesser Himalaya), bedload samples from mountain tributaries were collected in Tibet (Tsangpo drainage), Bhutan (Manas drainage), and Sikkim (Tista drainage; Fig. 1).

Over 300 grains were counted on each sample by the Gazzi–Dickinson method [21,22]. Dense minerals were concentrated with sodium metatungstate (density 2.9 g/cm^3), using the 63–250-μ

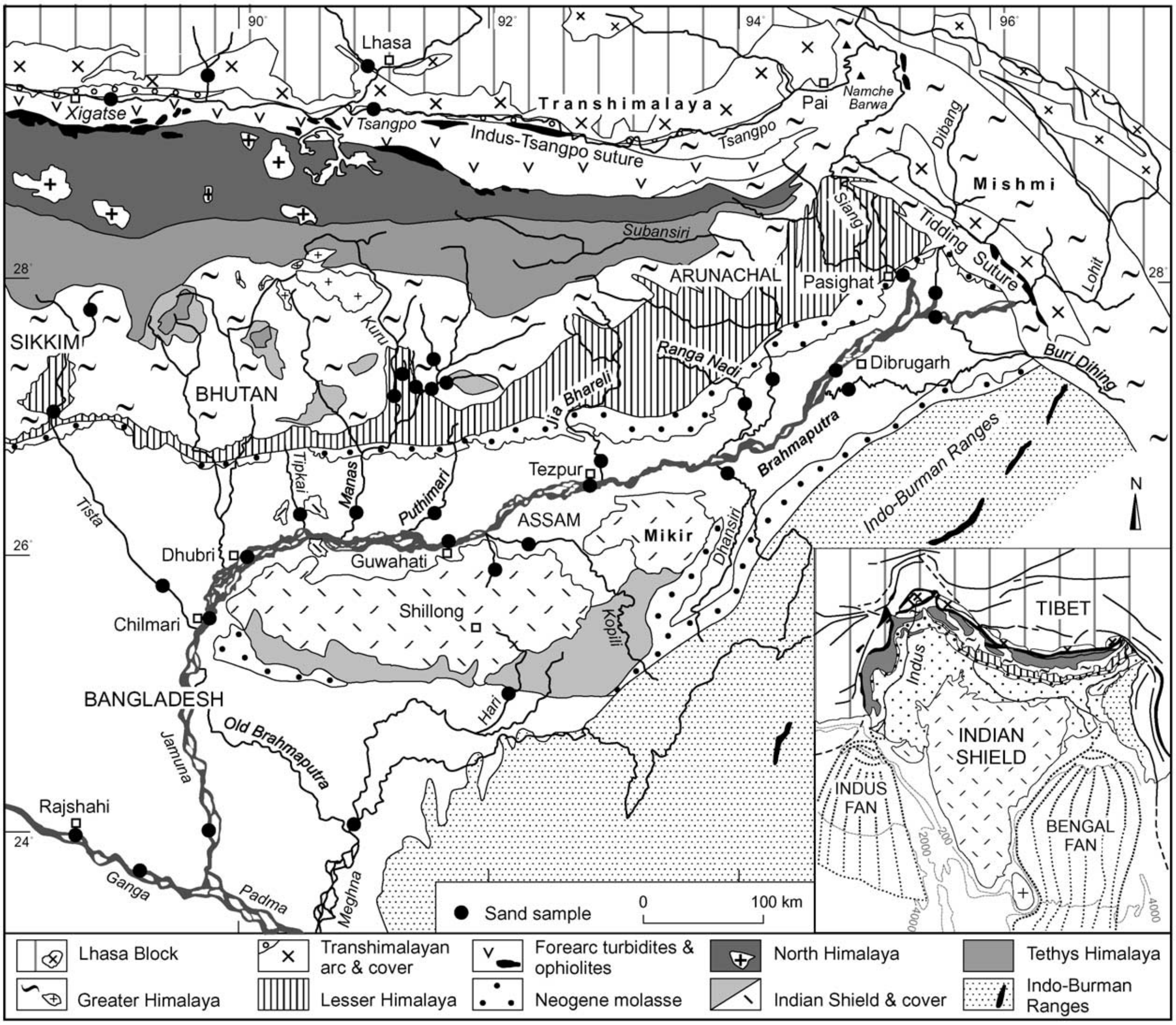

Fig. 1. Geologic sketch map (after [33] and other sources cited in text), indicating studied tributaries of the Brahmaputra River, and sampled sites.

fraction treated with oxalic and acetic acids. Detailed classification schemes allowed us to collect full quantitative information on framework grains and to recalculate a spectrum of primary proportional and secondary ratio parameters (Table 1 [19,23]). For diagrams shown in Figs. 2–6, 90% confidence regions about the mean were calculated with a statistically rigorous method devised specifically for compositional data [24].

2.2. Mixing model and sediment budget calculations

Relative contributions from each tributary to various segments of the trunk river were calculated by forward mixing models. Sand compositions can be expressed as mixtures of a fixed number of endmembers. The perfect mixing can be expressed as: $X = MB$, where X represents the matrix of compositional data, with n rows (samples)

Table 1
Recalculated key indices for framework composition and dense-mineral suites

Framework composition (QFL%) – Gazzi–Dickinson method	
Q	quartz
F	feldspars (Or = orthoclase/perthite; Mic = microcline; P = plagioclase)
Lv	volcanic and subvolcanic lithic fragments
Lc	carbonate lithic fragments (including marble)
Lp	terrigenous lithic fragments (shale, siltstone)
Lch	chert lithic fragments
Lm	metamorphic lithic fragments
Lu	ultramafic lithic fragments (serpentinite, foliated serpentineschist)
L = Lv+Lc+Lp+Lch+Lm+Lu = total aphanitic lithics (crystal size < 62.5 μ)	
Rank of metamorphic grains	
Rm0	unmetamorphosed sedimentary and volcanic to subvolcanic rock fragments
Rm1	very low-rank metamorphic rock fragments (rough cleavage, illite-chlorite)
Rm2	low-rank metamorphic rock fragments (strong cleavage, sericite)
Rm3	medium-rank metamorphic rock fragments (schistosity, tiny micas)
Rm4	high-rank metamorphic rock fragments (new crystals < 62.5 μ, muscovite)
Rm5	very high-rank metamorphic rock fragments (new crystals > 62.5 −, biotite)
Rm = Rm1+Rm2+Rm3+Rm4+Rm5	
MI = Rm1/Rm × 100+Rm2/Rm × 200+Rm3/Rm × 300+Rm4/Rm × 400+Rm5/Rm × 500	
Dense minerals (DM%)	
ZTR	ultrastable minerals (zircon, tourmaline, rutile)
A	amphiboles
Px	pyroxenes
O	olivine
S	spinel
Ep	epidote-group minerals
Gt	garnet
HgM	high-grade metamorphic minerals (staurolite, andalusite, kyanite, sillimanite)
&	other minerals (mostly sphene or chloritoid)

and p columns (variables). B represents the matrix of endmember compositions, and M the matrix of the proportional contribution of each endmember to each sample. The compositional variables are non-negative, and each row of the data matrix sums to a constant c (e.g., 100 for measurements recorded as percentages). If we assume that the compositional variation results from a physical mixing process, each sample of the matrix X is a non-negative linear combination M of the q rows of B [25].

These calculations, being flawed by various sources of potential error and depending on a variety of assumptions, are non-unique and uncertain. The results obtained in several independent trials were averaged, and 1σ standard deviation indicated. Dense minerals, being supplied by various source terranes in concentrations that differ by an order of magnitude, were treated separately. Given the large number of variables (26 significant mineral species), estimates are relatively precise, and proved to be essential in testing the overall consistency of the results obtained. Because suspended load fluxes are known with large uncertainties (± 50% for the Brahmaputra [9,10]), and bedload fluxes undetermined, calculations of sediment yields and denudation rates are highly tentative.

3. Focused erosion in the Himalaya

Even in presence of uniform convergence and steady-state input of crustal material into the thrust belt [26], erosion rates are heterogeneous over the Himalayan orogen [6,27]. The spatial distribution of detrital production and evacuation primarily relates to sharp local changes in slope amplified by very large discharges, and thus reflects the complex interplay between topography, climate, drainage patterns, and tectonic processes [7]. Most physical erosion takes place along the steep southern flank of the belt, drenched by summer-monsoon rains, where very high river gradients correspond to active uplift at the front of Greater Himalayan units [28].

Close relationships between river drainages and exhumation of deep structural levels within erosional windows and half-windows are observed all along the Himalayan arc, but the most spectacular examples occur at the eastern and western syntaxial terminations of the belt. Here two big rivers, the Tsangpo and the Indus, leave elevated Tibetan lands in the rain shadow of the Himalaya, to turn sharply south and cut impressive gorges transverse to the structural grain of crustal-scale antiforms, where metamorphic rocks up to granulite facies and Pleistocene anatectic granites are exposed. Spatial association between big-river gorges and crustal folds where mid-crustal rocks are quasi-instantaneously exhumed has suggested the existence of positive feedback between erosion and uplift of hot weak rocks from depth ('tectonic aneurysms' of [5]).

4. The Brahmaputra basin

The Tsangpo–Siang–Brahmaputra drainage basin ($\sim$630 000 km^2) is subdivided into three main parts with strongly contrasting elevation, relief, and climate. The Tibetan part, with average altitude of $\sim$4700 m above sea level (a.s.l.), covers a third of the total area ($\sim$220 000 km^2). Arid conditions on the plateau, in the shadow of the summer monsoon, generate a rainfall of only 0.3 m/yr, and the Tsangpo discharge upstream of Namche Barwa is $<$10% of the Brahmaputra flux in Bangladesh [29]. The Himalayan part of the drainage basin ($\sim$120 000 km^2) is exposed to heavy rainfall, particularly in the east ($\sim$2 m/yr). Alluvial plains in Assam and Bangladesh cover $\sim$200 000 km^2 of the area; the rest is drained by the Dibang and Lohit rivers ($\sim$50 000 km^2) and by southern tributaries. Himalayan, eastern, and southern tributaries represent 35%, 11% and 8% of total water discharge, respectively. Rainfall in Assam ranges 2–3 m/yr, and produces one third of total discharge [29]. No dams exist along the Brahmaputra, which is still a natural system. In Bangladesh, the river is called Jamuna. Southeast-directed until 1797 (Old Brahmaputra), it now runs southward, receives the Ganga River, and finally reaches the Bay of Bengal with a tidally influenced terminal tract named Padma or Meghna (Fig. 1).

4.1. The Tsangpo

The Tsangpo, originating in southwestern Tibet, flows eastward with low gradients for $\sim$1200 km along the southern boundary of the Tibetan Plateau. The upper course largely drains turbidites and ophiolitic mélange of the Indus–Tsangpo suture zone, which separates Indian outer-continental margin from Transhimalayan fore-arc basin sequences (Fig. 1). Its right (southern) tributaries drain the north face of Greater Himalayan peaks, Paleozoic to Eocene strata of the Tethys Himalayan zone, and North Himalayan gneiss domes [30]. Its left tributaries drain Transhimalayan gabbroic to granodioritic batholiths (Gangdese belt). The Lhasa block farther north includes Precambrian orthogneisses and metasediments, overlain by Carboniferous to Cretaceous strata and Paleogene ignimbrites [31].

4.2. The Siang

East of Pai ($\sim$3000 m a.s.l.), the Tsangpo swings around the eastern syntaxis through the deepest gorge on Earth, walled by Giala Peri (7281 m) and Namche Barwa peaks (7756 m), and plunges towards Arunachal Pradesh (India), where it is named Siang or Dihang. Extremely steep slopes particularly in the first 100 km of the gorge (30 m/km [32]), impressive landslides, and terraces incised by more than 350 m testify to extreme fluvial incision rates, inferred to be unsurpassed in the Himalayas and 1.4–3.7 times greater than the next largest ones in the Indus gorge [7]. Rapid fluvial incision leads to huge sediment fluxes, produced by the combination of extraordinary river gradients with the large water discharge fuelled by heavy summer-monsoon precipitation.

At the core of the Namche Barwa syntaxis, a northeast-plunging crustal-scale antiform, migmatitic Indian plate gneisses have been exhumed from below the Transhimalayan belt over the last 4 Ma. Peak metamorphic conditions at upper amphibolite to granulite facies (720–760°C, 8–10 kb) were reached at $\sim$16 Ma. Onset of decompression, with the last anatectic event recorded at 3.9–3.3 Ma, was followed by fast exhumation, with rates decreasing from 10 mm/yr at 3.5–3.2 Ma to 3–5 mm/yr since 2.2 Ma [32]. Folded around the syntaxis are Paleozoic to Mesozoic quartzites, phyllites and marbles that surround calc-alkaline plutons of the Transhimalayan belt. Intervening lenses of metabasites and serpentinites mark the eastern continuation of the Indus–Tsangpo suture [33].

In Arunachal Pradesh, the Siang River turns sharply southeastward, and cuts across the Lesser Himalayan and Sub-Himalayan zones to exit the mountains at Pasighat (~170 m a.s.l.). From north to south, Lesser Himalayan units include medium- to low-grade quartzites and schists with associated gneisses, lower greenschist-facies quartzites, carbonates and phyllites, very low-grade Permo-Carboniferous sandstones and shales, basalts (Abor Volcanics), and Eocene strata [34].

4.3. The Brahmaputra

The Brahmaputra is primarily a braided river, reaching a width up to 18 km and a depth of 35 m; water discharge, strongly dependent on summer-monsoon rains, varies annually from 3950 m^3/s (20/2/1984) to 76 500 m^3/s (18/9/1984 [35]). The river bed is locally directly superposed on Precambrian basement of the Shillong Plateau, which crops out only 30 km south of the Himalayan front without an intervening well-developed foreland basin.

The Shillong Plateau, reaching 2534 m a.s.l., is a pop-up structure uplifted by 6–7 km in the Plio-Quaternary along seismically active reverse faults [36]. As the adjacent Mikir Hills, it consists of amphibolite-facies gneisses, overlain in the south by gently dipping Cretaceous basalts (Sylhet Traps) and Tertiary shelf sediments.

Northern tributaries joining the Brahmaputra in Assam largely drain Himalayan metamorphic rocks, exposed in most of Bhutan. Only a few major rivers (Subansiri, Kuru) have their headwaters in the Tethys Himalayan sedimentary zone of south Tibet. The Greater Himalayan zone includes staurolite- to sillimanite-bearing schists and gneisses, diopside-bearing banded marbles, and locally amphibolites. Within this ~15-km-thick nappe-stack, metamorphic grade increases from lower amphibolite facies at the base to granulite facies at the top, where migmatites and Miocene leucogranites are most common. Exposed in several synforms are staurolite-grade to greenschist-facies calcschists, overlain locally by weakly metamorphosed fossiliferous strata and interpreted to be klippen of the Tethyan zone [37].

Himalayan tributaries in their lower course cut through the strongly deformed Lesser Himalayan zone. Quartzites and schists are widely exposed in the inner Lesser Himalaya, particularly in the Darjeeling and Shumar half-windows crossed by the Tista and Kuru rivers. Orthogneiss bodies and dolerite sills occur. Tertiary metamorphism reaches up to lower amphibolite facies in the footwall of the Main Central Thrust [38].

Precambrian dolostones, shales and quartzites exposed in the outer Lesser Himalaya mainly display lower greenschist facies. Younger anchimetamorphic units, exposed in the hanging wall of the Main Boundary Thrust, include pebbly mudrocks and Permo-Carboniferous quartzose sandstones, coal, and tillites [38]. Finally, the discontinuous Sub-Himalayan belt, accreted in the Quaternary along the Main Frontal Thrust, includes up to 3–4-km-thick Neogene molasse (Siwalik Group). Tilted gravel terraces and steep fault scarps document continuing uplift and deformation at the front of the growing orogen [39].

Eastern tributaries of the Brahmaputra (Lohit, Dibang) drain the Mishmi Hills, which include a calc-alkaline diorite–tonalite–granodiorite complex and tholeiitic metavolcanic rocks of island-arc affinity. They represent the prolongation of the Transhimalayan plutonic belt, and continue farther south into Burma/Myanmar. The Dibang and Lohit rivers next cut trough the Tidding suture, including chlorite-schists, amphibolites, serpentinites and metacarbonates, and finally across the easternmost continuation of the Himalayan belt [40].

Southern tributaries of the Brahmaputra (Buri Dihing, Dhansiri, Kopili) drain the outer part of the northern Indo-Burman Ranges. This accretionary prism, including Cretaceous–Eocene pelagic sediments overlain by thick Eocene–Oligocene turbidites associated with ophiolitic allochthons, was emplaced onto the eastern India shelf during mid-Tertiary oblique collision with southeast Asia [41].

5. Composition of Brahmaputra sands

5.1. Tibetan tributaries and the Tsangpo

Right tributaries of the Tsangpo, draining Te-

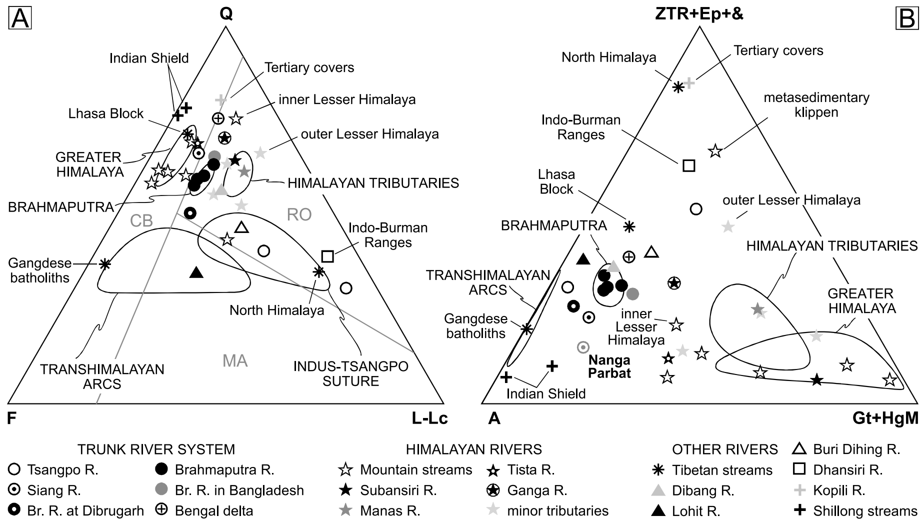

Fig. 2. Petrography (A) and mineralogy (B) of Brahmaputra sands. Indices explained in Table 1. (A) Trunk-river sands change abruptly around the eastern Himalaya syntaxis from lithic (Tsangpo) to quartzofeldspathic (Siang), next reflect mixing with feldspar-rich detritus from Mishmi arc rocks (Lohit), and finally remain constant across Assam (Brahmaputra), indicating subordinate contribution from Himalayan tributaries. Fields for Himalayan sands after [46]; 'continental block' (CB), 'recycled orogen' (RO), and magmatic arc (MA) fields after [22]. (B) Brahmaputra sands, as Siang sands and detritus from Nanga Parbat [46], are hornblende-dominated, and contrast sharply with garnet-rich sands of Himalayan tributaries.

thys and North Himalayan zones, carry abundant sedimentary and metasedimentary lithic grains, chloritoid from gneiss domes [42], and recycled ultrastables (mostly tourmaline). Left tributaries draining Gangdese arc batholiths carry plagioclase-dominated arkosic detritus, blue-green hornblende, and minor sphene, epidote, diopside, and hypersthene (Fig. 2). Rivers draining the Lhasa block carry quartzofeldspathic sands with blue-green hornblende, zircon, sphene, epidote, and garnet.

The Tsangpo sand at Xigatse is quartz-poor and dominated by shale/sandstone to slate/metasandstone grains from outer-continental margin and forearc basin turbidites, with subordinate detritus from ophiolitic mélanges. Dense minerals include epidote, hornblende, garnet, tourmaline, chloritoid, sillimanite, pyroxenes, and trace lawsonite. The Tsangpo sand south of Lhasa is enriched in quartz, feldspars, and blue-green hornblende from arc batholiths.

5.2. Siang River

Detrital modes change drastically around Namche Barwa, and the Siang sand at Pasighat shows a quartzofeldspathic signature, indicating provenance chiefly from mid-crustal rocks exposed in the eastern Himalayan syntaxis. Dolostone and metabasite grains are significant. Dense minerals are enriched in garnet at the expense of epidote with respect to Tsangpo sands (Table 2).

5.3. Himalayan tributaries

Detritus in Bhutan and Sikkim mountain rivers draining the high-grade, high-relief northern part of the Greater Himalaya consists of quartz, feldspars, very high-rank metamorphic rock fragments, abundant micas (10–15% of detritus, with dominant biotite), largely green-brown hornblende, garnet, and sillimanite. The Kuru River, sourced in the Tethyan zone, carries lower quartz and common terrigenous/slate to sparite/metacarbonate grains. Dense minerals include garnet, staurolite and diopside from amphibolite-facies metasediments.

As rivers cross-cut lower-grade units in the southern part of the belt, quartz and lower-rank metamorphic lithic fragments increase at the ex-

Table 2
Petrography and mineralogy of modern Brahmaputra sands

	N	% QFL								tot	P/F	MI	DM%	% DM								tot
		Q	F	Lv	Lc	Lp	Lch	Lm	Lu					ZTR	A	Px	O+S	Ep	Gt	HgM	&	
Tsangpo basin (Tibet)																						
Tsangpo @ Xigatse	1	29	7	1	5	34	1	22	2	100	40	143	3	9	23	11	0	29	15	5	7	100
Tibetan mountain tributaries	3	46	30	1	4	1	0	17	0	100	59	311	6	12	43	3	0	15	4	0	22	100
Tsangpo @ Gonggar	1	39	20	4	3	14	0	18	2	100	57	193	3	4	59	9	0	21	3	1	3	100
Himalayan tributaries																						
Bhutan mountain tributaries	6	61	26	0	1	1	0	11	0	100	46	402	10	6	32	3	0	13	30	14	1	100
Sikkim mountain tributaries	2	65	30	0	0	0	0	4	0	100	51	440	7	3	28	4	0	3	41	20	1	100
Subansiri	2	64	16	2	1	2	1	15	0	100	47	283	21	1	19	4	0	4	57	14	0	100
Manas	2	59	15	0	3	1	0	22	0	100	41	293	4	10	23	3	0	13	33	17	1	100
Tista	1	68	20	0	0	0	0	11	0	100	44	372	4	5	45	3	0	8	25	13	1	100
Ganga	4	66	14	0	6	2	0	12	0	100	47	289	2	7	36	9	0	19	19	6	3	100
Minor Himalayan tributaries	4	59	18	1	0	4	0	17	0	100	45	242	4	10	26	2	0	14	39	8	2	100
Left tributaries																						
Dibang	1	53	22	0	4	1	0	20	0	100	58	307	31	3	51	2	0	31	12	0	1	100
Lohit	1	32	37	1	6	1	0	22	0	100	74	342	45	0	57	1	2	36	4	0	1	100
Buri Dihing	1	46	23	0	0	4	3	23	1	100	54	261	7	0	34	10	6	32	14	1	1	100
Dhansiri	1	38	7	0	0	17	1	37	0	100	48	125	1	12	20	3	0	43	12	4	8	100
Kopili	1	80	11	0	0	3	0	6	0	100	24	224	2	59	10	0	0	20	3	2	6	100
Shillong tributaries	2	77	21	0	0	1	0	1	0	100	36	420	5	4	78	9	0	1	5	0	2	100
Trunk river																						
Siang @ Pasighat	1	61	21	0	8	0	0	9	0	100	46	334	18	6	58	9	1	11	10	2	4	100
Brahmaputra @ Dibrugarh	1	50	32	1	1	1	0	14	1	100	62	330	14	2	62	5	0	20	5	2	2	100
Brahmaputra @ Tezpur	2	60	25	0	0	1	0	13	0	100	46	297	9	2	51	3	0	25	16	0	3	100
Brahmaputra @ Guwahati	2	62	21	0	1	1	0	14	0	100	53	312	16	3	54	3	0	28	10	0	2	100
Brahmaputra pre-Tista	3	59	27	1	0	1	0	12	0	100	50	304	10	3	55	4	0	24	10	2	2	100
Brahmaputra pre-Ganga	2	65	20	0	0	0	0	14	0	100	51	279	20	2	51	1	0	22	17	2	5	100
Bengal Delta	3	72	14	0	3	2	0	8	0	100	44	274	12	2	46	2	0	32	12	2	4	100

N = number of samples. DM% = percent dense minerals in the analyzed very fine to fine sand fraction. Other indices as in Table 1.

pense of feldspars, and epidote and ultrastables become significant. Lower amphibolite-facies Lesser Himalayan rocks in the footwall of the Main Central Thrust shed quartzolithic detritus with common biotite and muscovite (9% of detritus), blue-green hornblende, and garnet. Metasedimentary klippen shed medium-rank metamorphic detritus and epidote-dominated assemblages including tourmaline, blue-green hornblende, garnet, and staurolite. Minor Himalayan tributaries draining the front of the belt (Ranga Nadi, Puthimari, Tipkai) carry pelite/sandstone to low-rank metapelite/metapsammite lithic fragments, and minor muscovite and biotite (3% of detritus). Garnet, kyanite, and staurolite, recycled from Sub-Himalayan molasse, are associated with ultrastables, epidote, and hornblende.

Major Himalayan tributaries (Subansiri, Manas, Tista) carry quartz, feldspars, metamorphic grains, and abundant micas (up to 23% of detritus, with dominant biotite). Dense minerals include hornblende, garnet, epidote, staurolite, kyanite, and sillimanite. The Ganga sands are similar, including more carbonate grains and epidote, and less garnet and high-grade minerals.

5.4. *Mishmi and Indo-Burman tributaries*

Eastern Assam rivers carry arkosic to quartzolithic sands derived in different proportions from the Himalayan, Mishmi, and Indo-Burman belts. At one extreme, the plagioclase-rich Lohit sand contains metapsammite, metabasite, and limestone grains, along with blue-green hornblende and epidote, indicating provenance chiefly from Mishmi arc plutons and amphibolites. At the other extreme, the feldspar-poor Dhansiri sand largely consists of shale/siltstone to slate/metasiltstone grains from accreted turbidites of the Indo-Burman Ranges; epidote prevails over blue-green hornblende, ultrastables, garnet, chloritoid, and staurolite. The Dibang sand includes metasedimentary, metabasite, and dolostone grains, along with blue-green hornblende, epidote and garnet, indicating mixed supply from Himalayan and Mishmi sources. The Buri Dihing sand includes terrigenous to very low-rank metasedimentary grains from accreted turbidites of the Indo-Burman Ranges, chert and ultramafic grains from ophiolitic sequences, epidote, hornblende, garnet, actinolite, diopside, enstatite, olivine, and spinel.

5.5. Shillong tributaries

Short streams draining the Shillong Plateau carry quartzofeldspathic detritus. Commonly pitted, embayed, or rounded quartz grains and low P/F ratio with abundant microcline indicate chemical weathering in tropical soils, and local recycling of terrigenous cover sequences. Dense minerals are dominated by blue-green to green-brown hornblende. Basaltic to diabase grains and clinopyroxenes from the Sylhet Traps occur locally (Hari, Meghna), as well as laterite soil clasts.

The Kopili River, flowing between the Mikir Hills and the Shillong Plateau, carries quartzose sandy silts including dominant zircon and other ultrastables. Recycling from terrigenous cover sequences [43] is indicated by commonly rounded quartz grains, high Q/F and very low P/F ratios. Terrigenous to low-rank metapelite/metapsammite lithic fragments from the Indo-Burman Ranges are minor.

5.6. Brahmaputra River

Brahmaputra sands maintain their petrographic and mineralogical signature across Assam. Subordinate supply by successive Himalayan tributaries is indicated by only slight decrease in metabasite grains and rank of metamorphic grains, and by persistently dominant hornblende, with invariably minor garnet, high-grade minerals, and tourmaline. The sharp decrease in Q/F ratio recorded at Dibrugarh, as well as the enrichment in epidote and zoisite from the Lohit confluence to the Bay of Bengal, indicate significant detritus from Mishmi sources.

6. Sediment budgets

Because the compositional signatures of various sources of detritus are known (Fig. 2), sediment budgets can be assessed directly from point-counting data with forward mixing models [25]. Such estimates, based on data from very fine- to coarse-grained bedload sands, may not be applicable to the mud fraction (suspended load). Also, they suffer from imprecision related to limited sample number and intrinsic variability of natural phenomena, and are based on several assumptions which are never strictly verified, including lack of mechanical destruction, chemical dissolution, hydraulic sorting, and recycling across the plains. Sediment transport cannot be envisaged as steady state, because detritus transported from uplands to sea is subject to a repeated series of depositional, burial, and erosional events induced by episodic flooding and channel migration [44].

The effects of downstream variations in sediment textures and compositional fractionation (e.g., detritus in suspension upstream which becomes part of the bedload downstream; lithic grains getting less abundant as sediments get finer) may be considered minor for the Brahmaputra River, which shows little downstream fining upstream of Bangladesh (correction coefficient not significant at the 10% level). Errors were minimized by analyzing, wherever possible, duplicate samples collected in different seasons, and by mutually constraining the two independent estimates obtained from petrographic and mineralogical data.

6.1. Budgets based on detrital modes

Detrital modes are consistent with a sediment contribution from the Siang River to the total Brahmaputra flux (pre-Tista confluence) estimated at $42 \pm 12\%$. Inferred contributions from Himalayan and Mishmi (chiefly Lohit) tributaries amount to $25 \pm 7\%$ and $20 \pm 2\%$, respectively. Contributions from the Shillong Plateau ($11 \pm$

5%) and Indo-Burman Ranges (~1%) are subordinate.

Our sample set is insufficient to accurately assess the supply from different Himalayan units to the Siang sand. We estimate contributions of ~75% from high-grade rocks exposed in the Namche Barwa syntaxis, the rest being provided in subequal amounts from Tibet (Tsangpo) and from Lesser and Sub-Himalayan units.

Intermediate composition of sands carried by Himalayan tributaries (Q/F 4.0 ± 1.6) with respect to detritus from the Greater (Q/F 1.8 ± 0.2) and Lesser Himalaya (Q/F > 7) indicates that Greater Himalayan rocks contribute little more than half of total bedload (Fig. 3). Dominant low-rank metamorphic grains in minor Himalayan tributaries (MI < 260; Ranga Nadi, Jia Barheli, Puthimari, Tipkai) and inverse correlation between rank of metamorphic grains and abundance of stable microcline with respect to total feldspars (correction coefficient −0.86, significance level 0.1%) show that very low-grade outer Lesser Himalaya metasediments and Neogene molasse represent important sources of sediment. This suggests intense fluvial incision at the front of the Himalaya, where rivers are forced to cut down to compensate for active thrusting and folding [45].

6.2. Budgets based on dense minerals

Dense minerals, even though influenced by hydraulic sorting, provide important complementary information. Their concentration varies strongly from one river to another, and this must be taken into account while integrating provenance budgets calculated from petrographic and mineralogical data. Dense minerals are most abundant in Dibang and Lohit sands derived from Mishmi plutons (DM% 31 and 45, respectively) or in trunk-river sands of Bangladesh (DM% 30–34), and most scarce in Puthimari and Dhansiri sands, derived from sedimentary to very low-grade metasedimentary rocks (DM% ≤ 1). The Siang (DM% 18), Subansiri (DM% 12–31) and Kuru rivers (DM% 28) carry much more dense minerals

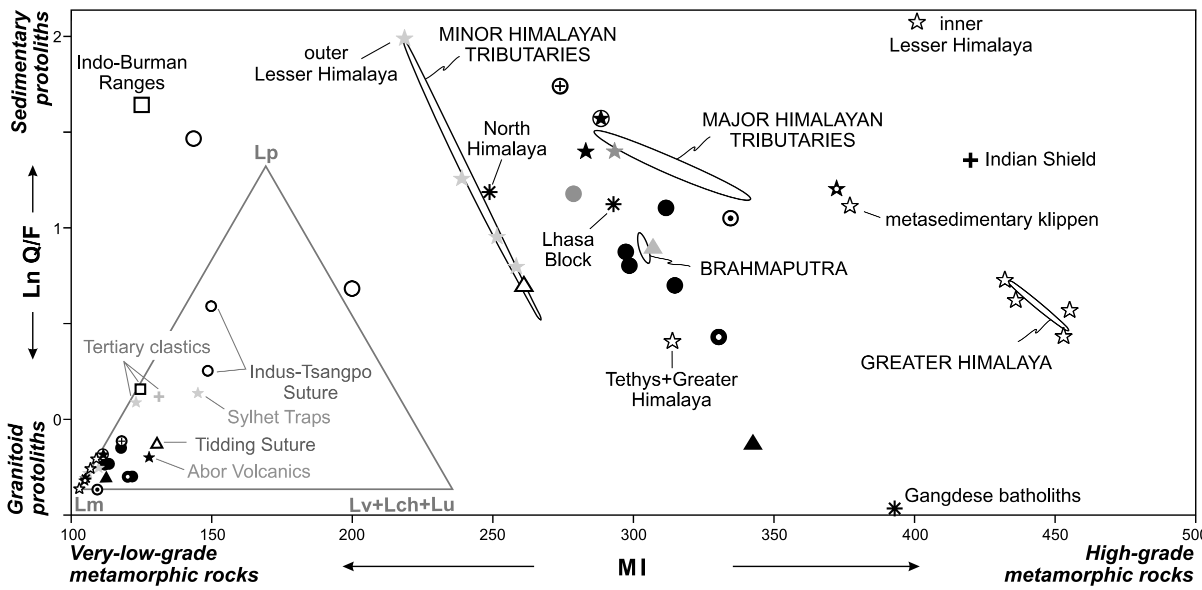

Fig. 3. Provenance of Brahmaputra sands. Detritus consists of quartz, feldspars and metamorphic lithic grains, with negligible contributions from volcanic and ophiolitic rocks ('collision orogen provenance' [19]). The Q/F ratio tends to decrease with increasing rank of metamorphic rock fragments (MI index [23]). Major Himalayan rivers (Ganga, Tista, Manas, Subansiri, Siang) carry abundant low-grade metasedimentary grains, suggesting active erosion of the growing mountain front. Indices explained in Table 1. Legend as in Fig. 2.

than the Tsangpo and other Himalayan or Shillong tributaries (DM% 4 ± 2). Dense minerals are markedly more abundant in Brahmaputra sands across Assam (DM% 11 ± 3) than in sands of major Himalayan tributaries (DM% 3.5 ± 1; Manas, Tista, Ganga).

Dense-mineral data are consistent with a contribution from the Siang River to the total Brahmaputra flux (pre-Tista confluence) estimated at $31 \pm 8\%$. Inferred contributions from Himalayan and Mishmi (chiefly Lohit) tributaries amount to $9 \pm 3\%$ and $52 \pm 4\%$, respectively. Contributions from the Shillong Plateau ($8 \pm 5\%$) and Indo-Burman Ranges ($< 1\%$) are subordinate.

Relative contributions from different Himalayan units to the Siang assemblage cannot be calculated accurately for both lack of samples and similar mineralogy of Tsangpo and Siang sand. Similar features are observed around the western Himalayan syntaxis, where the Indus sand in Ladakh and detritus from the Nanga Parbat Massif have virtually identical mineralogy to the Tsangpo and Siang sand, respectively [46]. We conclude that the Siang assemblage is compatible with dominant contribution from the eastern Himalaya syntaxis, with additional supply from Transhimalayan batholiths and minor ultrastables recycled from sedimentary and very low-grade metasedimentary rocks of the Lesser Himalayan and Sub-Himalayan zones.

Dense minerals in Himalayan tributaries are mainly supplied by Greater Himalayan units ($\sim 65\%$) and subordinately by lower-grade Lesser Himalayan units ($\sim 35\%$).

6.3. Bulk-sediment budgets

Because replicate samples could not be collected for the Siang and Lohit rivers, dense-mineral concentrations in Siang and Lohit sands are insufficiently constrained to obtain a robust integrated bulk-sediment budget. Our best estimates, calculated from the entire petrographic and mineralogical data set, suggest that the Siang River provides $\sim 41\%$ of total Brahmaputra flux (pre-Tista confluence), whereas Mishmi, Himalayan, Shillong, and Indo-Burman tributaries provide ~ 24, ~ 23, 11, and $\sim 1\%$, respectively. Such estimates compare with those based on geochemical data, which indicate a contribution of $49 \pm 27\%$ by the Siang to the Brahmaputra flux and dominant contributions of Greater Himalayan units to the Siang ($\sim 80\%$ [18]). Petrographic, mineralogical, and geochemical data thus consistently indicate that fast erosion around the Namche Barwa syntaxis contributes $35 \pm 6\%$ of the Brahmaputra sediment flux.

6.4. The Ganga–Brahmaputra Delta

Relative contributions of the Brahmaputra, Tista, Ganga, and Meghna rivers to the final sediment discharge into the Bay of Bengal cannot be estimated quantitatively from our petrographic and mineralogical data set. Decreasing grain size and hydraulic factors in Bangladesh cause an increase in quartz and marked variation of dense-mineral signatures and concentrations. Fluvial to marine sands downstream of the Brahmaputra–Ganga confluence vary from quartzofeldspathic (indicating Brahmaputra affinity) to quartzolithic with significant carbonate grains (suggesting Ganga affinity). Dense-mineral assemblages vary, with increasing dense-mineral concentration, from amphibole-dominated to rich in denser epidote and garnet. High epidote/garnet ratio [47] and low diopside indicate predominance of the Brahmaputra over the Ganga, which is hardly surprising because average dense-mineral concentration in Brahmaputra sands is four times higher than in Ganga sands.

6.5. The Bengal Fan

Bengal Fan sediments are quartzofeldspathic [14], with hornblende-dominated dense-mineral assemblages [15,17]. In spite of significant contribution by the Ganga River [18], detrital modes are quite close to Brahmaputra sand and dense-mineral assemblages are even richer in amphiboles. This suggests that cleavable feldspars and amphiboles are enriched in the suspended load and concentrated in the deep sea, whereas quartz and densest grains (garnet, epidote) tend to be segregated in the bedload and trapped on the coastal plain. Similar trends are observed for the

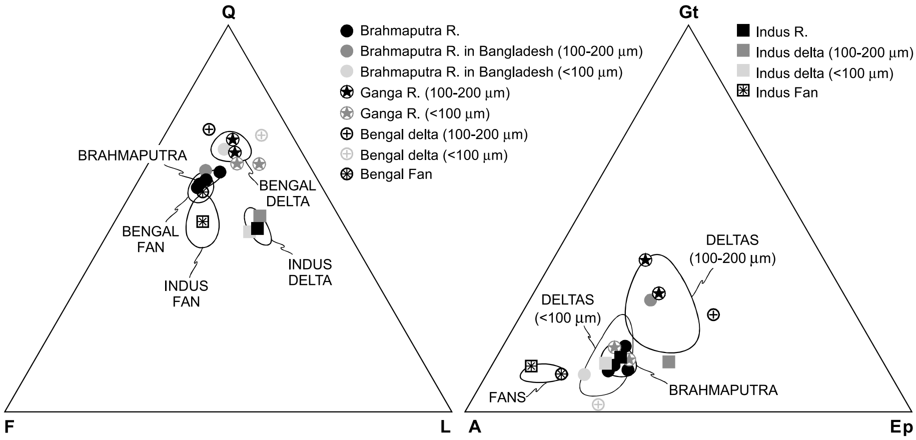

Fig. 4. The effect of hydraulic sorting. Grain size-related compositional changes are minor in Brahmaputra sands across Assam, but become significant in Bangladesh, where they dim provenance signatures and hamper calculation of sediment budgets. In the Bengal Delta, silty sands (grain size <100 μm) tend to be enriched in amphiboles. Conversely, clean sands (grain size >100 μm) are typically richer in garnet and epidote. Entrapment of coarser-grained sediments on the coastal plain can explain concentration of cleavable feldspars and lighter amphiboles in deep-sea turbidites (data after [14,15] for Bengal Fan, and after [16,46,60] for Indus Delta and Fan). Note similar sand composition in Brahmaputra and Indus systems, draining Tibet and cutting across Nanga Parbat and Namche Barwa syntaxes. Different abundance in lithics largely reflects increasing dissolution of carbonate grains from arid Pakistan to wet eastern India. Indices explained in Table 1.

Indus Delta and Fan (Fig. 4). More petrographic and mineralogical information is required to fully understand hydraulic sorting effects in deltaic to turbidite systems.

7. The effect of focused erosion

Independent estimates based on petrographic, mineralogical, and geochemical [18] data consistently indicate that the Brahmaputra sediment budget is dominated by the Siang River, with the Himalayan and Mishmi tributaries playing a significant but subordinate role. In turn, the Siang sediment flux is dominated by contributions from the Namche Barwa area ($\sim$27 000 km^2 [18]), representing only $\sim$11% of the Tsangpo–Siang basin and only $\sim$4% of the total Tsangpo–Siang–Brahmaputra basin.

This implies that the Namche Barwa syntaxis is eroding not only incomparably faster than south Tibet, but also much faster than the rest of the Greater Himalaya. Even if bedload fluxes (which are certainly large) are ignored, and a total Brahmaputra detrital flux of 780 ± 370 million tons/yr is conservatively considered [9,10], the Siang flux ($\sim$41%) would total 320 ± 152 million tons/yr, with a sediment yield from Namche Barwa of 8900 ± 4300 tons/km^2/yr, and denudation rates of 3.6 ± 1.7 mm/yr. These figures are consistent with exhumation rates of 4 ± 1 mm/yr since 2.2 Ma for Namche Barwa, calculated from thermochronological data on exposed bedrock [32]. Our estimates thus fully support the conclusions of [7], who calculated much higher erosion potential for the eastern Himalayan syntaxis than for anywhere else in the Himalaya.

Partitioning of Brahmaputra flux according to our estimates implies minimum sediment yields of 3700 ± 1800 tons/km^2/yr for the Mishmi Hills, of 1900 ± 900 tons/km^2/yr for the Himalaya west of the Siang Valley, of 2400 ± 1200 tons/km^2/yr for the Shillong Plateau, and of only 200 ± 100 tons/km^2/yr for Tibet, corresponding to minimum average denudation rates of 1.5 ± 0.7, 0.8 ± 0.4, 1.0 ± 0.5, and $\leq$ 0.1 mm/yr, respectively. Such sediment yields and denudation rates correlate strongly with precipitation and topographic gradients [8], but very poorly with elevation, as observed at the scale of the whole Himalaya [6,7]. Specifically, estimated erosion rates in the eastern syntaxis, drained by the powerful Siang River, are nearly five times higher than in Himalayan drainage basins to the west, lying in the rain shadow of the Shillong Plateau. This highlights the major role played in erosional systems by high water discharge. High precipitation and runoff in mountain areas enhance at the same time bedrock incision, rapid mass transfer through landsliding, and fluvial transport [48,49], while high relief is maintained by positive feedback between efficient evacuation of detritus and tectonic uplift [5]. It is noteworthy that much higher sediment fluxes are recorded in the eastern Himalayan syntaxis, where glacier erosion plays a subordinate role, than in highly glaciated areas around the western Himalayan syntaxis [50].

7.1. From Namche Barwa to Bengal Fan

According to our estimates, focused erosion of the eastern Himalayan syntaxis produces a sediment flux of 240 ± 115 million tons/yr, comparable to sediment discharge of the whole Indus River. If the Brahmaputra contributes ∼60% of the total sediment flux to the Bay of Bengal [9,10], focused erosion of Namche Barwa provides 21 ± 4% of the total budget of the largest sediment transport system on Earth. If exhumation rates of Namche Barwa were more than twice as high in the Pliocene [32], nearly a third of the upper portion of the Bengal Fan consists of detritus from the eastern Himalayan syntaxis. This is consistent with similar petrographic and mineralogical signatures of modern Siang sand and Plio-Quaternary Bengal Fan sediments [14,15]. Specifically, we tentatively interpret here the distinct increase in hornblende observed at mid-Pliocene times at Sites 218, 717, 718, and 719 as related to onset of rapid exhumation of the Namche Barwa syntaxis (Fig. 5). This tectonic process may have been triggered by capture of the Tsangpo drainage by the Brahmaputra River at ∼3.5 Ma [51].

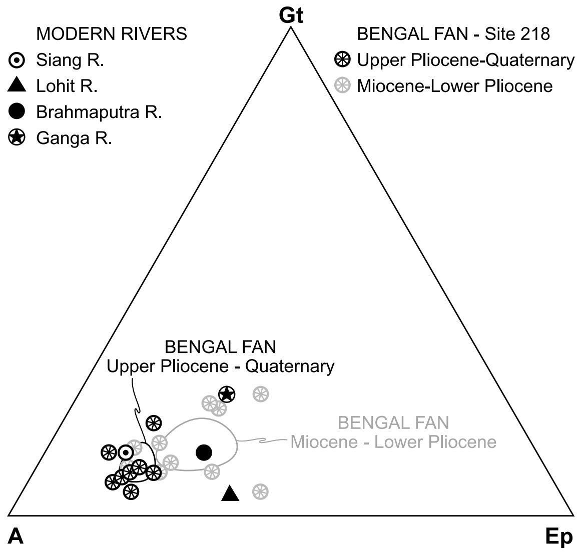

Fig. 5. The effect of focused erosion. Bengal Fan turbidites show a shift (at ∼300 m core depth, DSDP Site 218; data after [15]) from Brahmaputra-like mineralogy in the Miocene–Lower Pliocene to Siang-like mineralogy in the Upper Pliocene–Quaternary. This shift coincides with onset of fast growth and denudation of Namche Barwa antiform at ∼3.5 Ma [32]. Relative contributions to Bengal Fan through time from young metamorphic massifs (Siang sand), Transhimalayan batholiths (Lohit sand), and Himalayan belt (Ganga sand) cannot be quantified directly because of hydraulic sorting effects (Fig. 4). Amphiboles (A), epidote (Ep), and garnet (Gt), the three most abundant dense minerals in 'collision orogen provenance' [19], sum up to >70% of the dense fraction in all plotted samples.

8. The effect of chemical weathering

Sediment composition can be modified by numerous processes during erosion, transport, pedogenesis, recycling, final deposition, and diagenesis [52]. Studies investigating climatic control on petrology of modern sands have focused on semi-arid to humid areas of relatively low relief [53–55]. In high-relief settings, physical erosion typically prevails over chemical weathering, as observed even in humid monsoonal climates of northeastern India. However, stages of reduced transport, increasing residence time of sediments in the foreland basin, and more effective pedogenesis may lead not only to dissolution of carbonate grains but also to incongruent weathering of unstable silicates [6].

8.1. Himalayan tributaries

Even though limestones and marbles are significant in Tethys and Greater Himalayan units, respectively, carbonate and metacarbonate grains in fluvial sands are rare and mostly dolostone-dominated. In wet monsoonal climates, carbonate dissolution takes place even in mountain segments, as indicated by geochemical data [6,27]. Conversely, plagioclase/feldspar (P/F) ratios do not change significantly from mountain streams to the Assam plains, even though Lesser Himalayan and Sub-Himalayan sediments and metasediments are being actively recycled at the Himalayan front (Fig. 6). There is thus no indication of selective destruction of plagioclase with respect to the more stable K-feldspar. Clinopyroxenes are not more altered than amphiboles. Negligible chemical weathering is confirmed by only trace abundance of secondary minerals such as kaolinite and smectite in the suspended load [18].

8.2. Assam plains

Dolostone and limestone grains (carried not only by the Tsangpo draining arid Tibet but also by major Himalayan and Mishmi rivers including the Siang, Dibang, Lohit, and Manas) are lacking in Brahmaputra sands, documenting complete dissolution in the monsoon-drenched Assam plains. Olivine (present in trace in Siang, Lohit, and Buri Dihing sands) is also lacking. Nearly half of pyroxenes (derived from Greater Himalayan metacarbonates, from arc and ophiolitic sequences of the Indus–Tsangpo and Tidding su-

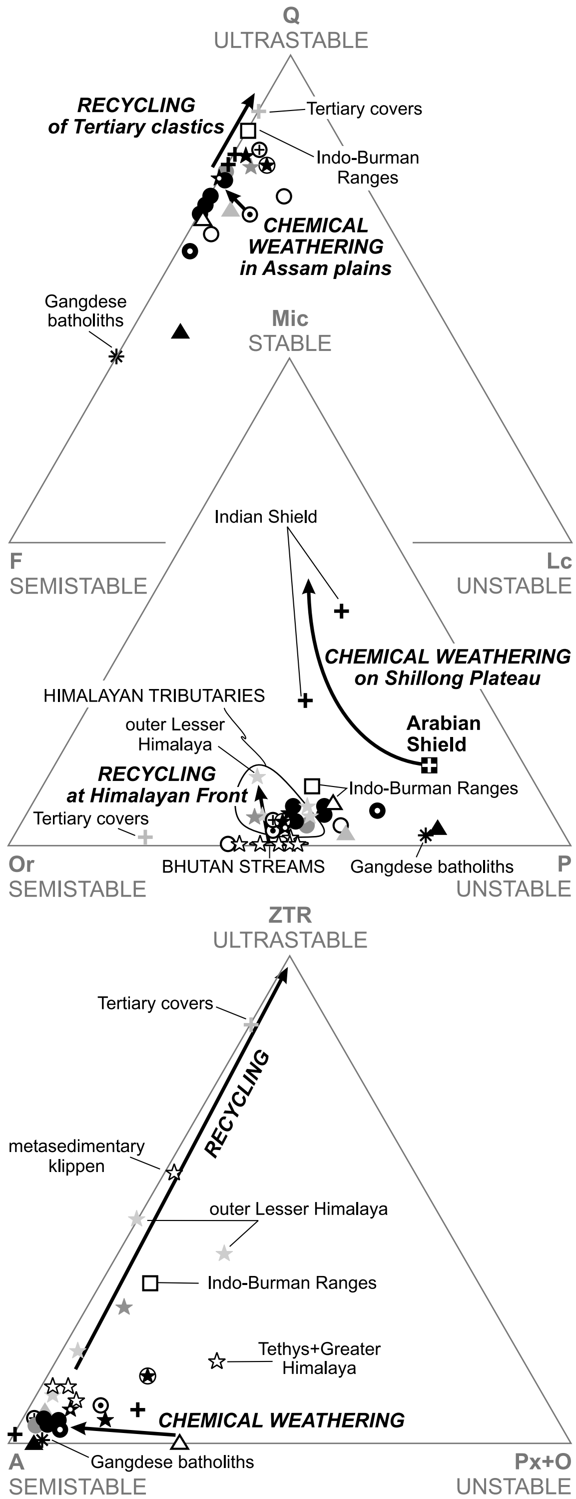

→

Fig. 6. The effect of chemical weathering. Dissolution in Assam plains is documented by lack of carbonate and olivine grains and by commonly etched pyroxene. Instead, constant P/F ratio and dominant fresh hornblende indicate no selective destruction of plagioclase or amphibole. Strong chemical weathering in soils is testified only by marked enrichment in microcline in detritus from Shillong Plateau (data for Arabian Shield after [57]). Increasing microcline and ultrastable minerals from Bhutan and Sikkim mountain rivers to Himalayan tributaries in Assam, without any significant decrease in P/F ratio, indicates recycling of very low-grade metasediments and molasse across the actively-uplifted front of the Himalaya. Recycling of Tertiary clastic rocks explains high quartz and ultrastable minerals, as well as low P/F ratio or relative abundance of microcline, in Kopili and Dhansiri sands. Note similarity of Lohit sand with detritus from Gangdese arc batholiths. Indices explained in Table 1.

tures, or from the Sylhet Traps) display incipient dissolution, indicating partial destruction during multistep transport. Pyroxenes are locally common in samples collected during the late-monsoon season, suggesting more rapid transport and limited reworking of previously-deposited sediments. Q/F ratios, P/F ratios, and hornblende-dominated dense-mineral assemblages remain remarkably constant, indicating no physical or chemical breakdown of feldspars and amphiboles (Fig. 6).

8.3. Shillong tributaries

Detritus from the Shillong Plateau, including commonly pitted and embayed quartz grains, low P/F ratio, abundant microcline, etched clinopyroxene, and laterite clasts, reveals the effect of pedogenesis in the source area. These features are typical of sediments derived from cratonic interiors in wet climates [56]. Climatic-induced modifications of detrital modes can be assessed by comparison with modern sands from the Arabian Shield, produced and deposited in hyperarid settings (Fig. 6 [57]). Best-fit calculations suggest that ∼80% of original plagioclase and lithic grains and 40–45% of original orthoclase-perthite grains have been selectively dissolved with respect to quartz and microcline, both assumed as chemically stable. This is the maximum effect which can be ascribed to chemical weathering, assuming no recycling of cover sandstones. Significant but not extreme weathering with complete feldspar dissolution, as observed for sediments derived from the Brazilian and Guyana shields [58,59], is indicated.

9. Conclusions

The Brahmaputra is the big-river basin with the highest denudation rates on Earth [8]. Erosion, far from being evenly distributed, is very low in 2/3 of the basin, including the elevated Tibetan Plateau and the Assam to Bangladesh plains. Erosion rates vary strongly even along the Greater Himalayan belt, and reach peaks nearly five times higher in the eastern syntaxis than in Himalayan regions to the west.

Independent calculations based on petrographic, mineralogical, and geochemical [18] data on the same sample set suggest that the Namche Barwa area, representing only ∼4% of total basin area, contributes 35 ± 6% of the total Brahmaputra sediment flux; Tibet, with an area of ∼1/3, contributes only 5%. Within the Himalayan belt west of Namche Barwa, detritus derives in subequal proportions from Greater Himalayan units and lower-grade Lesser and Sub-Himalayan units.

The Siang River, draining the syntaxis, contributes ∼25% of total sediments reaching the Bay of Bengal (not much less than the ∼40% represented by the four times larger Ganga basin); 14% each derives from Himalayan tributaries and from the Mishmi Hills (mainly via the Lohit River), and the remaining 7% from the Shillong Plateau and Indo-Burman Ranges. The Siang contribution to total sediment budget is such that the distinct mineralogical change recorded within mid-Pliocene turbidites of the Bengal Fan may be interpreted as reflecting onset of fast erosion of the Namche Barwa antiform at ∼3.5 Ma, with denudation rates up to 10 mm/yr [32].

The Himalayan belt, where rainfall increases markedly from west to east, is an ideal site in which to evaluate climatic control on sediment composition. Given the extreme erosion rates and rapid transport of detritus, detrital modes display minor traces of chemical weathering in mountain streams. In contrast, sand-sized carbonate grains are lacking and pyroxene selectively altered across monsoon-drenched Assam plains. Selective destruction of either plagioclase or amphibole is not observed. Only detritus from the Shillong Plateau is depleted in unstable feldspars and enriched in microcline, indicating intense weathering. Carbonate grains are found in Ganga sands and become common in Indus sands, indicating that climatic effects decrease progressively westward across the Indo-Gangetic foreland.

Most difficult to assess is the effect of hydraulic sorting in deltaic settings. Denser minerals (garnet, epidote) are enriched in coarser sediments trapped on the coastal plain. Cleavable feldspars and amphiboles are concentrated in the finer fraction, and preferentially deposited in the deep sea.

This study stresses the importance of focused erosion in alpine-type mountain belts. Close relationships between geology and drainage document coupling of tectonic and surface processes all along the Himalayan belt and in particular at both of the syntaxes, where uplift of the Tibetan Plateau has forced runoff from a vast elevated land to carve the two deepest river gorges on Earth. Such great irregularities in erosion patterns suggest that, even in presence of steady-state influx of crustal material [26], a steady-state cylindrical orogen can exist only in highly idealistic models.

Acknowledgements

The paper benefited from very careful reviews by P.G. DeCelles and B. Hallet. Our friends B. Lombardo, Y. Najman, I. Villa, and N. White provided several samples and shared their knowledge in many fruitful discussions through the years. S. Monguzzi and P. Paparella helped in the laboratory. C. Malinverno and M. Minoli made thin sections and drawings. The complete petrographical and mineralogical database is available from the corresponding author upon request. Financial support by FIRB 2002 and Cofin 2003 to E.G.***[KF]***

References

[1] J.D. Milliman, R.H. Meade, World delivery of river sediment to the oceans, J. Geol. 91 (1983) 1–21.
[2] G. Einsele, L. Ratschbacher, A. Wetzel, The Himalayan-Bengal Fan denudation-accumulation system during the past 20 Ma, J. Geol. 104 (1996) 163–184.
[3] P.D. Clift, N. Shimizu, G.D. Layne, J.S. Blusztajn, C. Gaedicke, H.-U. Schlüter, M.K. Clark, S. Amjad, Development of the Indus Fan and its significance for the erosional history of the western Himalaya and Karakoram, Geol. Soc. Am. Bull. 113 (2001) 1039–1051.
[4] J.P. Avouac, E.B. Burov, Erosion as a driving mechanism of intracontinental mountain growth, J. Geophys. Res. 101 (1996) 17747–17769.
[5] P.K. Zeitler, A.S. Meltzer, P.O. Koons, D. Craw, B. Hallet, C.P. Chamberlain, W.S.F. Kidd, S.K. Park, L. Seeber, M. Bishop, J. Shroder, Erosion, Himalayan geodynamics, and the geomorphology of metamorphism, GSA Today 11 (2001) 4–9.
[6] A. Galy, C. France-Lanord, Higher erosion rates in the Himalaya geochemical constraints on riverine fluxes, Geology 29 (2001) 23–26.
[7] D.P. Finlayson, D.R. Montgomery, B. Hallet, Spatial coincidence of rapid inferred erosion with young metamorphic massifs in the Himalayas, Geology 30 (2002) 219–222.
[8] M.A. Summerfield, N.J. Hulton, Natural controls of fluvial denudation rates in major world drainage basins, J. Geophys. Res. 99 (1994) 13871–13883.
[9] W.W. Hay, Detrital sediment fluxes from continents to oceans, Chem. Geol. 145 (1998) 287–323.
[10] M.R. Islam, S.F. Begum, Y. Yamaguchi, K. Ogawa, The Ganges and Brahmaputra rivers in Bangladesh: basin denudation and sedimentation, Hydrol. Process. 13 (1999) 2907–2923.
[11] S.L. Goodbred, S.A. Kuehl, Enormous Ganges-Brahmaputra sediment discharge during strengthened early Holocene monsoon, Geology 28 (2000) 1083–1086.
[12] P.E. Potter, Petrology and chemistry of modern big river sands, J. Geol. 86 (1978) 423–449.
[13] D.K. Datta, V. Subramanian, Texture and mineralogy of sediments from the Ganges-Brahmaputra-Meghna river system in the Bengal Basin, Bangladesh, and their environmental implications, Environ. Geol. 30 (1997) 181–188.
[14] R.V. Ingersoll, C.A. Suczek, Petrology and provenance of Neogene sand from Nicobar and Bengal Fans, DSDP Sites 211 and 218, J. Sediment. Petrol. 49 (1979) 1217–1228.
[15] R.W. Thompson, Mineralogy of sands from the Bengal and Nicobar fans, Sites 218 and 211, Eastern Indian Ocean, Initial Reports DSDP 22, 1974, pp. 711–713.
[16] T.K. Mallik, Mineralogy of deep-sea sands of the Indian Ocean, Mar. Geol. 27 (1978) 161–176.
[17] K. Yokohama, K. Amano, A. Taira, Y. Saito, Mineralogy of silts from the Bengal Fan, in: J.R. Cochran, D.A.V. Stow et al. (Eds.), Proc. ODP Sci. Res. 116, 1990, pp. 59–73.
[18] S.K. Singh, C. France-Lanord, Tracing the distribution of erosion in the Brahmaputra watershed from isotopic compositions of stream sediments, Earth Planet. Sci. Lett. 202 (2002) 645–662.
[19] E. Garzanti, G. Vezzoli, B. Lombardo, S. Andò, E. Mauri, S. Monguzzi, M. Russo, Collision-Orogen Provenance (Western and Central Alps): Detrital signatures and unroofing trends, J. Geol. 112 (2004).
[20] P.D. Clift, J.I. Lee, P. Hildebrand, N. Shimizu, G.D. Layne, J. Blusztajn, J.D. Blum, E. Garzanti, A.A. Khan, Nd and Pb isotope variability in the Indus River system: Implications for sediment provenance and crustal heterogeneity in the Western Himalaya, Earth Planet. Sci. Lett. 200 (2002) 91–106.
[21] R.V. Ingersoll, A.G. Kretchmer, P.K. Valles, The effect of sampling scale on actualistic sandstone petrofacies, Sedimentology 40 (1993) 937–953.
[22] W.R. Dickinson, Interpreting provenance relations from detrital modes of sandstones, in: G.G. Zuffa (Ed.), Prov-

enance of Arenites, ASI Series 148, Reidel, Dordrecht, 1985, pp. 333–361.
[23] E. Garzanti, G. Vezzoli, A classification of metamorphic grains in sands based on their composition and grade, J. Sediment. Res. 73 (2003) 830–837.
[24] G.J. Weltje, Quantitative analysis of detrital modes: statistically rigorous confidence methods in ternary diagrams and their use in sedimentary petrology, Earth Sci. Rev. 57 (2002) 211–253.
[25] G.J. Weltje, Provenance and dispersal of sand-sized sediments, Ph.D. Thesis, Universiteit Utrecht, 1994, 208 pp.
[26] R. Bendick, R. Bilham, How perfect is the Himalayan arc?, Geology 29 (2001) 791–794.
[27] N. Harris, M. Bickle, H. Chapman, I. Fairchild, J. Bunbury, The significance of the Himalayan rivers for silicate weathering rates: evidence from the Bhote Kosi tributary, Chem. Geol. 144 (1998) 205–220.
[28] L. Seeber, V. Gornitz, River profiles along the Himalayan arc as indicators of active tectonics, Tectonophysics 92 (1983) 335–367.
[29] K.L. Rao, India's Water Wealth, Orient Longman, New Delhi, 1979, 267 pp.
[30] J.-P. Burg, G.M. Chen, Tectonics and structural zonation of southern Tibet, China, Nature 311 (1984) 219–223.
[31] C. Chengfa et al., Preliminary conclusions of the Royal Society and Academia Sinica 1985 geotraverse of Tibet, Nature 323 (1986) 501–507.
[32] J.-P. Burg, P. Nievergelt, F. Oberli, D. Seward, P. Davy, J.-C. Maurin, Z. Diao, M. Meier, The Namche Barwa syntaxis: evidence for exhumation related to compressional crustal folding, J. Asian Earth Sci. 16 (1998) 239–252.
[33] A. Gansser, Ophiolitic belts of the Himalayan and Tibetan region, Geological Map 1:2,500,000, IGCP Project 'Ophiolites', Unesco, 1979.
[34] S. Singh, P.K. Chowdhary, An outline of the geological framework of the Arunachal Himalaya, J. Himal. Geol. 1 (1990) 189–197.
[35] C.S. Bristow, Brahmaputra River; channel migration and deposition, in: F.G. Ethridge, R.M. Flores, M.D. Harvey, J.N. Weaver (Eds.), Recent Developments in Fluvial Sedimentology, Soc. Econ. Paleontol. Miner. Spec. Publ. 39, 1987, pp. 63–74.
[36] R. Bilham, P. England, Plateau 'pop-up' in the great 1897 Assam earthquake, Nature 410 (2001) 806–809.
[37] D. Grujic, L.S. Hollister, R.R. Parrish, Himalayan metamorphic sequence as an orogenic channel: insight from Bhutan, Earth Planet. Sci. Lett. 198 (2002) 177–191.
[38] A. Gansser, Geology of the Bhutan Himalaya, Birkhauser, Basel, 1983, 181 pp.
[39] T. Nakata, Active faults of the Himalaya of India and Nepal, in: L.L. Malinconico, R.J. Lillie (Eds.), Tectonics of the Western Himalayas, Geol. Soc. Am. Spec. Pap. 232, 1989, pp. 243–264.
[40] G. Kumar, Geology of the Arunachal Pradesh, Geol. Soc. India, Bangalore, 1997, 217 pp.
[41] S. Sengupta, K.K. Ray, S.K. Acharyya, J.B. de Smeth, Nature and ophiolite occurrences along the eastern margin of the Indian plate and their tectonic significance, Geology 18 (1990) 439–442.
[42] J.-P. Burg, M. Guiraud, G.M. Chen, G.C. Li, Himalayan metamorphism and deformations in the North Himalayan Belt (southern Tibet, China), Earth Planet. Sci. Lett. 69 (1984) 391–400.
[43] L.L. Bhandari, R.C. Fuloria, V.V. Sastri, Stratigraphy of Assam Valley, India, Am. Assoc. Petrol. Geol. Bull. 57 (1979) 642–654.
[44] D.J. Stanley, A.K. Hait, Deltas, radiocarbon dating, and measurements of sediment storage and subsidence, Geology 28 (2000) 295–298.
[45] J. Lavé, J.P. Avouac, Fluvial incision and tectonic uplift across the Himalayas of central Nepal, J. Geophys. Res. 106 (2001) 26561–26591.
[46] E. Garzanti, G. Vezzoli, S. Andò, P. Paparella, Petrography and mineralogy of sediments from big Himalayan rivers, in: 18th Himalaya-Karakorum-Tibet Workshop, Ascona, 2003, pp. 46–50.
[47] D.C. Heroy, S.A. Kuehl, S.L. Goodbred, Mineralogy of the Ganges and Brahmaputra Rivers: implications for river switching and Late Quaternary climate change, Sediment. Geol. 155 (2003) 343–359.
[48] D.W. Burbank, J. Leland, E. Fielding, R.S. Anderson, N. Brozovic, M.R. Reid, R. Duncan, Bedrock incision, rock uplift and threshold hillslopes in the northwestern Himalayas, Nature 379 (1996) 505–510.
[49] N. Hovius, C.P. Stark, P.A. Allen, Sediment flux from a mountain belt derived by landslide mapping, Geology 25 (1997) 231–234.
[50] J.F. Shroder, M.P. Bishop, Unroofing of Nanga Parbat Himalaya, in: M.A. Khan, P.J. Treloar, M.P. Searle, M.Q. Jan (Eds.), Tectonics of the Nanga Parbat Syntaxis and the Western Himalaya, J. Geol. Soc. Lond. Spec. Publ. 170, 2000, pp. 163–179.
[51] M.E. Brookfield, The evolution of the great river systems of southern Asia during the Cenozoic India-Asia collision: rivers draining southwards, Geomorphology 22 (1998) 285–312.
[52] M.J. Johnsson, The system controlling the composition of clastic sediments, in: M.J. Johnsson, A. Basu (Eds.), Processes Controlling the Composition of Clastic Sediments, Geol. Soc. Am. Spec. Pap. 284, 1993, pp. 1–19.
[53] L.J. Suttner, A. Basu, G.H. Mack, Climate and the origin of quartz arenites, J. Sediment. Petrol. 51 (1981) 1235–1246.
[54] J.H. Grantham, M.A. Velbel, The influence of climate and topography on rock-fragment abundance in modern fluvial sands of the southern Blue Ridge Mountains, North Carolina, J. Sediment. Petrol. 58 (1988) 219–227.
[55] E. Le Pera, J. Arribas, S. Critelli, A. Tortosa, The effects of source rocks and chemical weathering on the petrogenesis of siliciclastic sand from the Neto River (Calabria, Italy): implications for provenance studies, Sedimentology 48 (2001) 357–378.
[56] H.W. Nesbitt, C.M. Fedo, G.M. Young, Quartz and feldspar stability, steady and non-steady-state weathering,

and petrogenesis of siliciclastic sands and muds, J. Geol. 105 (1997) 173–191.
[57] E. Garzanti, G. Vezzoli, S. Andò, G. Castiglioni, Petrology of rifted-margin sand (Red Sea and Gulf of Aden, Yemen), J. Geol. 109 (2001) 277–297.
[58] P.E. Potter, Modern sands of South America: composition, provenance and global significance, Geol. Rundsch. 83 (1994) 212–232.
[59] M.J. Johnsson, R.F. Stallard, R.H. Meade, First-cycle quartz arenites in the Orinoco River basin: Venezuela and Colombia, J. Geol. 96 (1988) 263–277.
[60] C.A. Suczek, R.V. Ingersoll, Petrology and provenance of Cenozoic sand from the Indus cone and the Arabian Basin, DSDP Sites 221, 222, and 224, J. Sediment. Petrol. 55 (1985) 340–346.